



Article

Identification and Characterization of *Heme Oxygenase-1* from *Litopenaeus vannamei* Involved in Antioxidant and Anti-Apoptosis under Ammonia Stress

Yongxiong Huang ^{1,†}, Qi Li ^{1,†} , Shiping Yang ^{1,2,3,*}, Yunhao Yuan ¹, Zhiqiang Zhang ¹ , Baijian Jiang ¹, Jing Lv ¹, Jian Zhong ³ and Jichang Jian ^{1,2,3,*}

- ¹ Guangdong Provincial Key Laboratory of Aquatic Animal Disease Control and Healthy Culture & Key Laboratory of Control for Diseases of Aquatic Economic Animals of Guangdong Higher Education Institutes, College of Fishery, Guangdong Ocean University, Zhanjiang 524094, China
- ² Guangdong Provincial Engineering Research Center for Aquatic Animal Health Assessment, Shenzhen 518116, China
- ³ Zhanjiang Customs District People's Republic of China, Zhanjiang 524000, China
- * Correspondence: ysp20010@sina.com (S.Y.); jianjc@gdou.edu.cn (J.J.)
- † These authors contributed equally to this work.

Abstract: Heme oxygenase-1 (HO-1) is a stress-inducible enzyme with antioxidant, anti-inflammatory, and anti-apoptotic effects. In this study, the *HO-1* gene from *Litopenaeus vannamei* (*Lv-HO-1*) was identified. The open reading frame of *Lv-HO-1* is 747 bp, encoding a peptide of 248 amino acids as well as a conserved HemO structural domain. *Lv-HO-1* is 70–90% homologous to crustaceans and about 50% homologous to arthropods. The transcript levels of *Lv-HO-1* were highest in the hepatopancreas and lower in other tissues. Knockdown of *Lv-HO-1* led to structural destruction of the hepatopancreas. After ammonia exposure, *Lv-HO-1* was significantly induced. Knockdown of *Lv-HO-1* during ammonia exposure resulted in a significant decrease in antioxidant capacity and cellular autophagy levels compared to the control and increased apoptosis. The transcriptional levels of *SOD* and *GSH-Px* were considerably reduced ($p < 0.05$), as were the transcriptional levels of *Atg3*, *Atg4*, *Atg5*, and *Atg10*. The results indicated that *Lv-HO-1* from *L. vannamei* can be induced by oxidative stress and may have important roles in regulating the host antioxidant system, reducing cell apoptosis.

Keywords: *HO-1*; RNA interference; *Litopenaeus vannamei*; oxidative stress; apoptosis; autophagy



Citation: Huang, Y.; Li, Q.; Yang, S.; Yuan, Y.; Zhang, Z.; Jiang, B.; Lv, J.; Zhong, J.; Jian, J. Identification and Characterization of *Heme Oxygenase-1* from *Litopenaeus vannamei* Involved in Antioxidant and Anti-Apoptosis under Ammonia Stress. *Fishes* **2022**, *7*, 356. <https://doi.org/10.3390/fishes7060356>

Academic Editor: Luisa María Vera

Received: 6 October 2022

Accepted: 25 November 2022

Published: 28 November 2022

Publisher's Note: MDPI stays neutral with regard to jurisdictional claims in published maps and institutional affiliations.



Copyright: © 2022 by the authors. Licensee MDPI, Basel, Switzerland. This article is an open access article distributed under the terms and conditions of the Creative Commons Attribution (CC BY) license (<https://creativecommons.org/licenses/by/4.0/>).

1. Introduction

The rate-limiting enzyme, heme oxygenase (HO), catalyzes the conversion of heme and generates the antioxidant products ferrous ion, carbon monoxide, and biliverdin [1]. The non-rate-limiting enzyme biliverdin reductase reduces the reaction product biliverdin to bilirubin [2,3]. HO has been found in insects, fish, and mammals, among other organisms [4]. There are three isoforms, HO-1, HO-2, and HO-3 [5]. HO-2 is a constitutively produced protein that has a role in a variety of physiological processes [6,7]. Functional investigations on HO-3 are still restricted and it was discovered to be an HO-2 pseudogene [8]. HO-1 is an inducible isoform [9] that is abundant in the liver and spleen, whereas lower levels were detected in the other tissues. As a stress-response protein [10], HO-1 can be highly induced by a variety of substances that cause oxidative stress. Hypoxia, inflammatory conditions, and endotoxins all stimulate HO-1, which protects cells from oxidation and cellular stresses while also reducing inflammation, apoptosis, and regulating cell proliferation [1,11,12].

In mammals, the function and regulation of *HO-1* have been studied using in vitro and in vivo models of oxidant-mediated cell and tissue injury [13]. The relevance of *HO-1* has been shown in numerous investigations. *HO-1* inhibits glucose-induced apoptosis in

human microvascular endothelial cells [14]. Under endotoxic circumstances, *HO-1* (–/–) mice were more likely to die or develop hepatic necrosis [15]. Studies have shown that *HO-1* is significantly induced in animal models of ischemia/reperfusion and nephrotoxin-induced acute kidney injury (AKI) [16,17]. Cisplatin medication of genetically deficient *HO-1* mice results in worse kidney function and tubular damage [18]. In fish, hypoxia increased the activity of *HO-1* in the gills of fish living in 7 °C. While *HO-1* was inhibited, the ventilation frequency response to acute hypoxia was enhanced [19]. Recent research on *Drosophila melanogaster* suggests that HO is involved in the regulation of essential apoptosis and autophagy processes in protecting the brain from oxidative damage [20]. However, the physiological control of *HO-1* in crustaceans has received less attention than in mammals, leaving a gap in our knowledge of the roles of *HO-1* in shrimp.

L. vannamei is an internationally known economic shrimp, widely farmed worldwide, especially in China. However, ammonia is the most common pollutant in aquaculture waters and is highly toxic to crustaceans, leading to oxidative stress [21] and an immune response [22]. High ammonia levels can seriously damage the hepatopancreas, induce apoptosis, and even lead to the death of shrimp [23]. We speculated that *Lv-HO-1* participates in the mediation of stress responses and cytoprotective effects in *L. vannamei*. Therefore, *Lv-HO-1* was identified and its properties and functions were investigated. These data may deepen our comprehension of the function of *HO-1* in shrimp and the regulatory mechanism of the invertebrate antioxidant system.

2. Materials and Methods

2.1. Shrimp Preparation, Challenge, and Sample Collection

L. vannamei (8.0 ± 0.5 g) were obtained and acclimated in seawater at 28.0 ± 0.5 °C and salinity of 30.0 ± 0.5 ‰ for 7 days. These shrimps were then randomly selected for the experiment. Three healthy shrimps were sampled to clone the *Lv-HO-1* gene and track its distribution in the brain, intestines, gills, epidermis, hepatopancreas, muscle, eyestalk, and hemolymph. Total RNA was extracted immediately.

The ammonia stress experiment was conducted as previously described [24]. Ammonium chloride reagent (Sigma, Shanghai, China) was used with a final concentration of 20 mg/L of ammonia-N added to seawater. After ammonia exposure, tissues of three shrimps were collected as described above at two time points (0, 48 h). Total RNA was extracted immediately.

2.2. RNA Isolation and cDNA Synthesis

RNAiso Plus (TaKaRa, Dalian, China) was used to isolate and extract total RNA from shrimp. The RNA was then extracted with chloroform, the supernatant was centrifuged and precipitated with isopropyl alcohol to obtain the RNA, and finally the RNA was dissolved with 50 µL of RNase-free water. RNA concentration was measured using NANODROP 2000 (Thermo Scientific) and RNA integrity was detected using 1.2% agarose gel. PrimeScript™ RT reagent Kit with gDNA Eraser (TaKaRa, Dalian, China) was used to reverse-transcribe the RNA following the kit instructions. The reverse-transcribed cDNA was diluted at a ratio of 1:50 for subsequent experiments [25,26].

2.3. Cloning and Sequence Analysis of *Lv-HO-1*

The predicted gene sequence of *Lv-HO-1* was obtained from NCBI and partial sequence primers of *Lv-HO-1* (*HO-1-S* and *HO-1-A*) were designed. The first strand of cDNA was then synthesized from the total mRNA as a polymerase chain reaction (PCR) template, and the *HO-1* fragment was amplified and sequenced. Using sequenced sequences, primers were designed for amplification of 5' terminal sequences (*HO-1-5'* RACE and *HO-1-5'* RACE nested) and 3' terminal sequences (*HO-1-3'* RACE and *HO-1-3'* RACE nested), respectively. Sequence-cloning methods were referenced to the SMARTer RACE 5'/3' kit instructions (Code No. 634858; Clontech, Mountain View, CA, USA). Eventually, the 3' RACE and 5' RACE sequences were spliced via contigExpress application assembly

software to derive the full length of the *HO-1* gene. Multiple sequence alignment of *HO-1* protein was performed via DNAMAN software (version 7.0, LynnonBiosoft, San Ramon, CA, USA). Neighbor-joining (NJ) phylogenetic trees with 1000 bootstrap replications were constructed using MEGA software (version 6.0, Philadelphia, PA, USA).

2.4. RNAi Assay

A set of primers with the T7 promoter sequence was generated based on the *HO-1* cDNA sequence and amplification of a fragment of about 500 bp. An exogenous control dsRNA (dsEGFP) fragment of 497 bp was amplified using primers for the enhanced green fluorescent protein (EGFP). The PCR products were in vitro transcribed using T7 RNAi Transcription Kit (Takara, China) to synthesize dsRNA. Double-stranded RNA was precipitated with ethanol after being extracted with chloroform/phenol. The quality and amount of dsRNA were assessed via 1.2% agarose gel electrophoresis and spectrophotometry. The abdomen intramuscular dsRNA was injected as shown below. The double-stranded RNA of *Lv-HO-1* was injected into each experimental shrimp at a rate of 0.50 µg/g. An identical amount of EGFP was injected into the control group. The hepatopancreas and muscle were sampled with three replicate samples at three different intervals (3, 5, and 7 days) after injection. Total RNA extraction was performed following the steps described in this section. The efficiency of RNAi was determined via qRT-PCR.

2.5. Ammonia Exposure Assay

The healthy shrimps were selected and randomly divided into 4 groups with 30 shrimps and raised in 100 L of seawater as mentioned above continuously for 3 weeks. For the blank group, each shrimp was injected with 30 µL of PBS. For dsRNA-EGFP and dsRNA-*Lv-HO-1* groups, 120 µg of dsRNA-EGFP and dsRNA-*Lv-HO-1* were each dissolved in 900 µL of PBS, and then injected into each shrimp separately. All three groups, excluding the blank group, were subjected to ammonia-N stress 3 days after the test and the final concentration of ammonia-N was 20 mg/L [24]. At 48 h after the exposure, hepatopancreas tissues from 3 shrimp were collected for total RNA extraction and histological analysis, respectively.

2.6. Quantitative Real-Time PCR (qRT-PCR)

Tissue distribution and relative expression of *Lv-HO-1* were examined by qRT-PCR to detect transcript levels in healthy shrimp. qRT-PCR was carried out utilizing TB Green® Premix Ex Taq™ II (Tli RNaseH Plus) (TaKaRa, Dalian, China) and QuantStudio 6 and 7 Flex Real-Time PCR Systems (Thermo Fisher Scientific, Waltham, USA). PCR (triplicated) consisted of 30 s at 95 °C followed by 40 cycles at 95 °C for 15 s, 60 °C for 30 s, and a melting curve assay at the end. A 184 bp fragment of the *Lv-HO-1* gene was amplified with *EF1α* as the internal reference gene. All primers used in this study are shown in Table S1 (Supplementary Materials). The relevant levels of *HO-1* were calculated via the $2^{-\Delta\Delta Ct}$ method [27].

2.7. Histologic Analysis

Hepatopancreas was fixed in a mixture of ethanol, chloroform, and glacial acetic acid with a volume ratio of 6:3:1 for more than 24 h in ethanol dehydrated using a gradient of ethanol (70%, 85%, 95%, and 100%), vitrified in xylene, and then embedded in paraffin. Hematoxylin and eosin staining kit (Beyotime, Shanghai, China) was used on serial 9 µm thick dewaxed and rehydrated sections. Histological analyses were stained using a hematoxylin and eosin staining kit (Beyotime, Shanghai, China) following the manufacturer's protocols. A Nikon DS-Ri2 camera was used for microscopic observation and photography (Nikon, Tokyo, Japan).

2.8. TUNEL Assay

One-step TUNEL Assay Kit (Green, FITC; Elabscience, Wuhan, China) was used to detect apoptosis. Hepatopancreatic cell apoptosis was detected by paraffin biopsy, accord-

ing to the manufacturer's instructions. The apoptotic cells were labeled with fluorescent dUTP and the cells were counter-stained with DAPI (blue) following the manufacturer's protocols. The section was examined by fluorescence microscopy.

2.9. Enzyme Activities Assays

The excised hepatopancreas was homogenized at 4 °C and separated at 5000× g for 30 min. The antioxidant parameters were measured directly from the supernatant fluids following the protocols of the kits (Nanjing Jiancheng Bioengineering Institute).

2.10. Drawings and Statistical Analysis

The data were presented using mean ± standard deviation (SD). One-way ANOVA and Student's *t*-test were used to analyze the significance of differences with Prism software (version 8.0). Homogeneity of variance test was performed prior to one-way ANOVA. Duncan's post-hoc was used when all variances were equal. Different lowercase letters denote significant differences between groups, ($p < 0.05$).

3. Results

3.1. Cloning and Bioinformatics Analysis of *Lv-HO-1*

The full length of *Lv-HO-1* cDNA is 913 bp with a 747 bp open reading frame (ORF) encoding 248 amino acids (Figure 1A). The predicted protein molecular weight of *Lv-HO-1* is 28.6 kDa with a theoretical *pI* of 6.55. Comparison of genomic sequences showed that *Lv-HO-1* consists of four exons separated by three introns (Figure 1B). Multiple sequence alignment revealed that the amino acid sequence of *Lv-HO-1* contains a conserved HemO structural domain. The inferred amino acid sequence of *Lv-HO-1* has similarities with *Lv-HO-1* from other species, according to Basic Local Alignment Search Tool (BLAST, NCBI) analysis. There was a 68–97% match with other shrimp species and a 10% match with vertebrates (Figure 2A). Phylogenetic analysis showed that *Lv-HO-1* originally clustered with *Penaeus monodon* and then with other crustaceans. Finally, *Lv-HO-1* clustered with vertebrates (Figure 2B).

3.2. Expression Characteristics of *Lv-HO-1* in Various Tissues

The expression of *Lv-HO-1* in various tissues was detected by qPCR. Among all the analyzed tissues, the *Lv-HO-1* mRNA level was highest in hepatopancreas then decreasingly in muscle, gill, epithelium, hemocytes, intestine, and brain (Figure 2C).

3.3. Effects of Ammonia Exposure on Expression of *Lv-HO-1*

The expression of *Lv-HO-1* was abundant in the hepatopancreas and muscle. The hepatopancreas is an important immune and metabolism organ, and muscle is the maximal tissue in *L. vannamei*. Therefore, the hepatopancreas and muscle were selected to detect the expression levels of *Lv-HO-1* during oxidative stress. After ammonia exposure, *Lv-HO-1* expression levels were considerably raised in hepatopancreas and muscle ($p < 0.05$). In addition, after stress, the *Lv-HO-1* transcript level peaked at 12 h and folded at 24 h in the hepatopancreas, while it peaked at 24 h and folded at 48 h in the muscle (Figure 3). These findings suggested that *Lv-HO-1* might play a role in antioxidants.

3.4. *Lv-HO-1* Silencing via RNAi

RNAi knockdown efficiency of *Lv-HO-1* was assessed using qPCR. The expression levels of *Lv-HO-1* in hepatopancreas and muscle were examined 3, 5, and 7 d after dsRNA injection. The expression level of *Lv-HO-1* was significantly decreased ($p < 0.05$) in the dsRNA-*Lv-HO-1* group compared to the PBS group, while the dsRNA-EGFP (Figure 4A) was not significantly different. RNAi in hepatopancreas had a higher silencing effectiveness than muscle, reaching a silencing efficiency of 70%. Therefore, RNAi is an effective way to reduce the expression of the *Lv-HO-1* gene. Hepatopancreas structures in the dsRNA-EGFP control and dsRNA-*LvHO-1* groups were different, as showed by sections stained with H&E.

Thinning and dilatation of the hepatic tubule wall were observed in the hepatopancreas of the dsRNA-*Lv-HO-1* group (Figure 4B). Meanwhile, the sections showed different levels of pathological changes under ammonia stress. Severe dilatation of the stellate tubular lumen and thinning were observed in the dsRNA-*Lv-HO-1* group but occurred only mildly in the dsRNA-EGFP group (Figure 4B).

A

```

1 gactaccaaagcagagtaaatctccggggaggagcttcagataaaaagacccaagctcct
1      M S S T E E V P F T K Q M R N
61 ttacattcagcaggATGTCTTCCACTGAAGAGGTGCCATTCACTAAACAAATGCGAAAT
16 V T R E I H N V S D A L I N A K L G I A
121 GTTACAAGAGAGATTACAAATGTCAGTGATGCATTGATAAATGCCAACTTGGAAATTGCC
36 M S E D R V W A E G L L I F Y E I F K Y
181 ATGTCAGAGGATCGAGTGTGGGCTGAAGGTCTCCTGATATTTATGAAATTTCAAATAC
56 L E E A L D R L S H T L I S D L D I P G
241 CTCGAAGAAGCTTTGGATAGACTCTCACACACCCCTTATAGTGATCTGGACATCCCAGGC
76 M R R K E A F E K D L A F Y L G S N W K
301 ATGAGGCGAAAGGAAGCTTTTGAAAAGGATTAGCATTCTATTAGGAGTAACTGGAAG
96 D G Y K P R E S V C Q Y L K H L E K I E
361 GACGGATACAAGCCAAGGGAGAGCGTATGCCAGTATTAAACACCTTGAGACATCGAG
116 Q E N P Y Y L M S Y I Y H L Y M G L L S
421 CAGGAAAATCCATACATCTTATGTCTTATATTTACCACTTGATACGGGGCTCTTATCT
136 G G Q I L R R K K V L L Q K F S F S R K
481 GCGCGCCAAATCTTGAGACGGAAGAAGGTCTTGCTACAAAAATTCCTTTTTCGTAAG
156 D S V E G M A V T E I D T S V S R L K R
541 GATTCTGTGGAAGGCATGGCAGTGACCGAGATTGATACTTCAGTATCCAGGTTGAAAAGG
176 E M T E A M N R I A E E L D E E T K Q R
601 GAGATGACAGAGGCCATGAATCGTATGCTGAGGAGCTCGATGAGGAGACGAAGCAGCGA
196 L L D E S K M V F I L N N S I V H S V E
661 CTTCTGGACGAGAGCAAGATGGTCTTCATTCTTAACAACAGTATTGTTCACTCAGTGGAA
216 G A G S V V A M K I L K F A S Y G V L S
721 GGAGCTGGTAGTGTGTGGCCATGAAAATCCTCAAGTTTGCTCTTATGGGGTCCTTTCT
236 A L L F V Y I K R M L V G *
781 GCATTATTATTGTTTACATTAAGAGGATGCTAGTAGGGTAaaaaagccttttggtgaag
841 ttgatgtaaatatgaacttagttggaggagcaagtgtacaggtgttatactgttctgtt
901 ccagttatttgaa

```

B

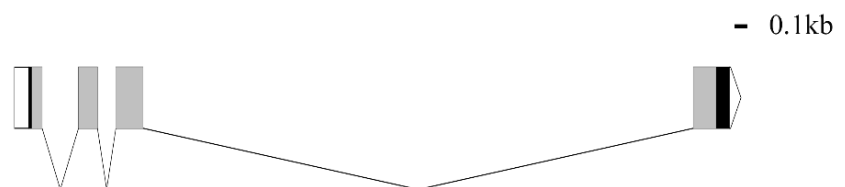


Figure 1. (A) cDNA sequences and deduced amino acid sequences of *Lv-HO-1*. The open reading frame (ORF) is capitalized. An asterisk indicates the stop codon. (B) Genomic structure of *Lv-HO-1* contains three introns and four exons. Untranslated sections are marked with a white box (UTR).

3.5. Effect of Silencing *Lv-HO-1* on Antioxidant Capacity

The expression levels of antioxidant-related genes and enzyme activities were also analyzed. The expression levels of *superoxide dismutase* (SOD) and *glutathione peroxidase* (GSH-Px) were significantly decreased ($p < 0.05$) in each group after ammonia exposure. In the dsRNA-*Lv-HO-1* group, the transcription levels of SOD and GSH-Px were significantly decreased compared with the PBS group (Figure 5A). Meanwhile, the enzyme activity of SOD in the dsRNA-*Lv-HO-1* group was also significantly decreased ($p < 0.05$) compared to the PBS group or dsRNA-EGFP group. The MDA level in the dsRNA-*Lv-HO-1* group was essentially increased ($p < 0.05$) compared with the PBS group or dsRNA-EGFP group. The activity of SOD in the dsRNA-*Lv-HO-1* group decreased by 35% while the MDA increased by 28% in comparison to the PBS group or dsRNA-EGFP group (Figure 5B).

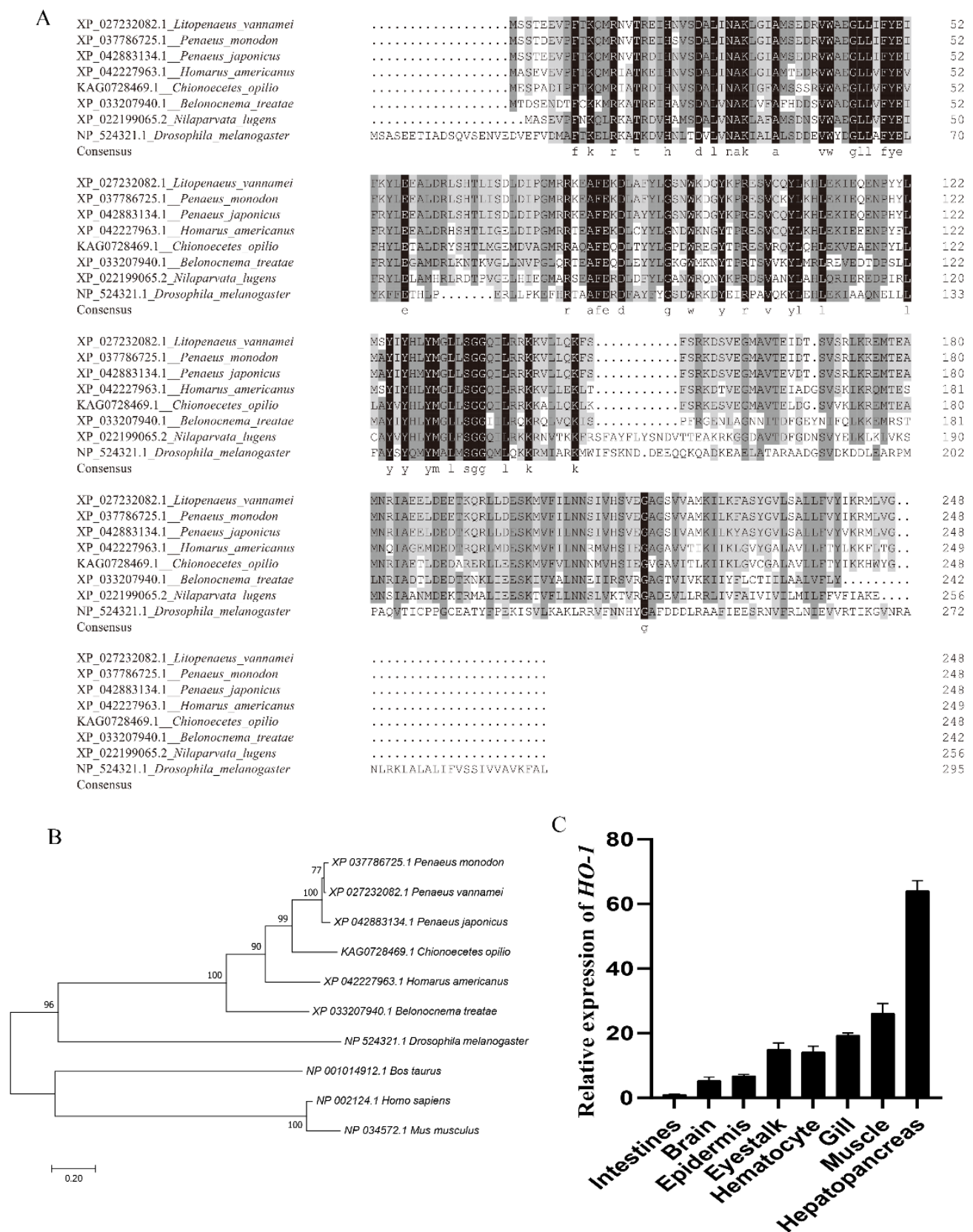


Figure 2. (A) Multiple alignments of the HO-1 sequence from various species. (B) Phylogenetic tree of the *Lv*-HO-1 family built via neighbor joining. (C) *Lv*-HO-1 levels in different tissues in *L. vannamei* were evaluated via qRT-PCR. All values are the mean \pm SD; $n = 3$.

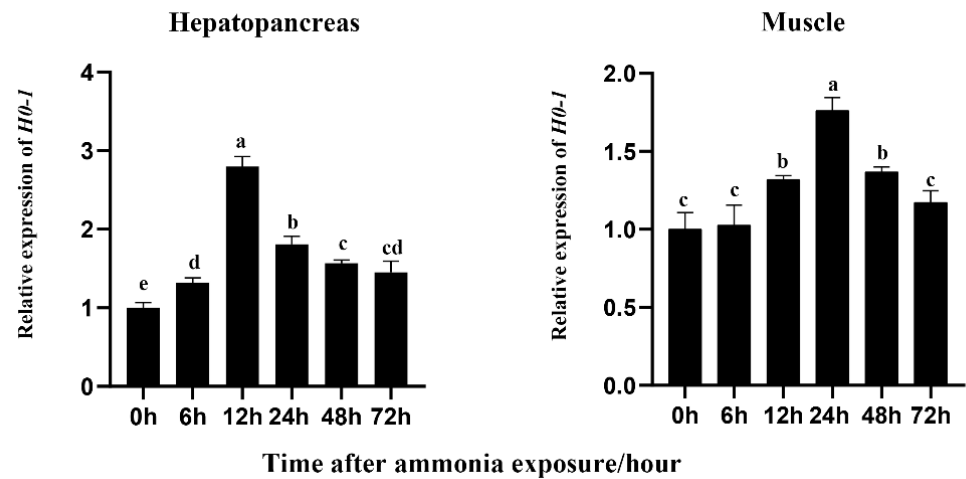
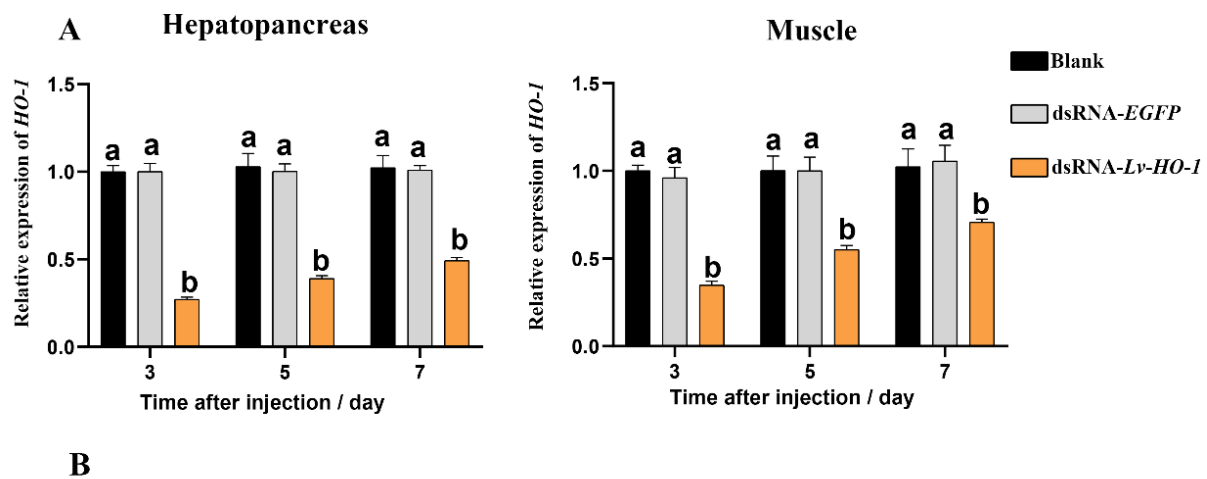


Figure 3. Transcription patterns of *Lv-HO-1* in hepatopancreas and muscle at different time points after ammonia-N stress. To determine the relative expression of the other time point, the *Lv-HO-1* expression level at 0 h was set to 1.00. All values are the mean \pm SD, $n = 3$. Different letters denote a significant difference ($p < 0.05$).



B

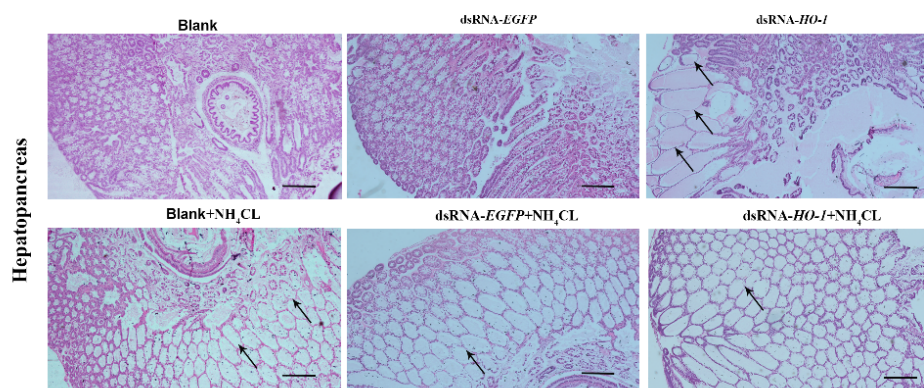


Figure 4. (A) Levels of *Lv-HO-1* mRNA in hepatopancreas and muscle after RNAi injection. Significant difference ($p < 0.05$) in the dsRNA-*Lv-HO-1* group compared with the Blank or PBS group is denoted by different letters. (B) Histological examination of hepatopancreas after RNAi. The sections were stained with H&E (50 \times magnification, Scale plate: 20 μ m). Arrows indicate thinning and dilatation of the hepatic tubule wall.

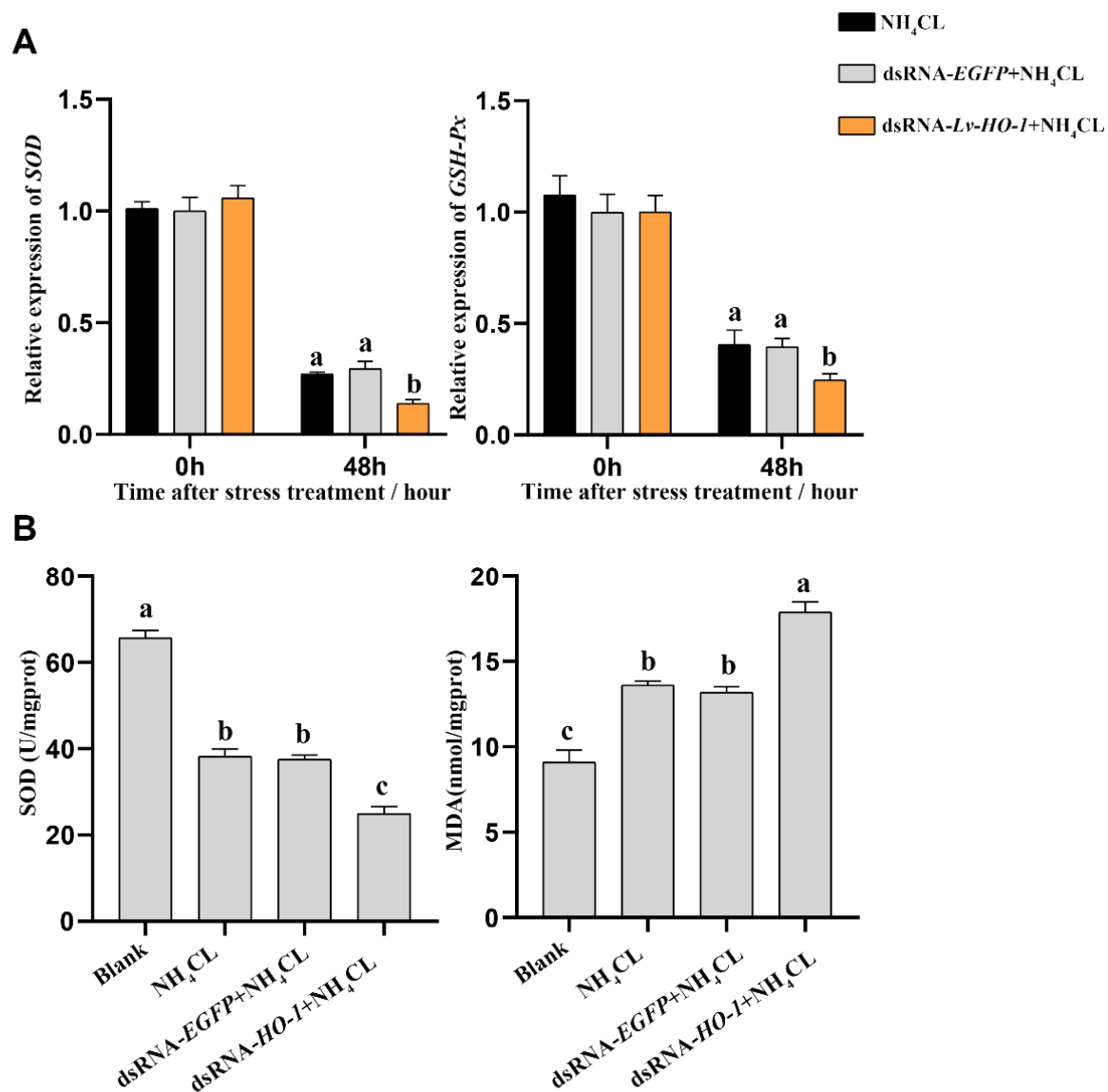


Figure 5. (A) *Mn-SOD* and *GSH-Px* in the hepatopancreas post-RNAi detected by qRT-PCR after ammonia-N stress. All values are the mean \pm SD; $n = 3$. (B) The activities of SOD and the content of MDA in the hepatopancreas after ammonia exposure. Different letters indicate a significant difference ($p < 0.05$).

3.6. Effect of Silencing *Lv-HO-1* on Autophagy and Apoptosis

Expression levels of autophagy genes including *Atg3*, *Atg4*, *Atg5*, and *Atg10* in the PBS and dsRNA-EGFP groups all increased after ammonia exposure. However, the expression levels of autophagy genes in the dsRNA-*Lv-HO-1* group were significantly decreased ($p < 0.05$) compared with the PBS or dsRNA-EGFP group after stress (Figure 6A). Similarly, the expression levels of apoptosis genes (*caspase 2* and *caspase 3*) significantly increased ($p < 0.05$). Remarkably, the expression levels of *caspase 2* and *caspase 3* in the dsRNA-*Lv-HO-1* group significantly increased ($p < 0.05$) compared with the PBS or dsRNA-EGFP group at 48 h (Figure 6B). The apoptosis signals are green and the apoptotic signal in the dsRNA-*Lv-HO-1* group was substantially higher than in the dsRNA-EGFP group while the blank group had no positive signal (Figure 7).

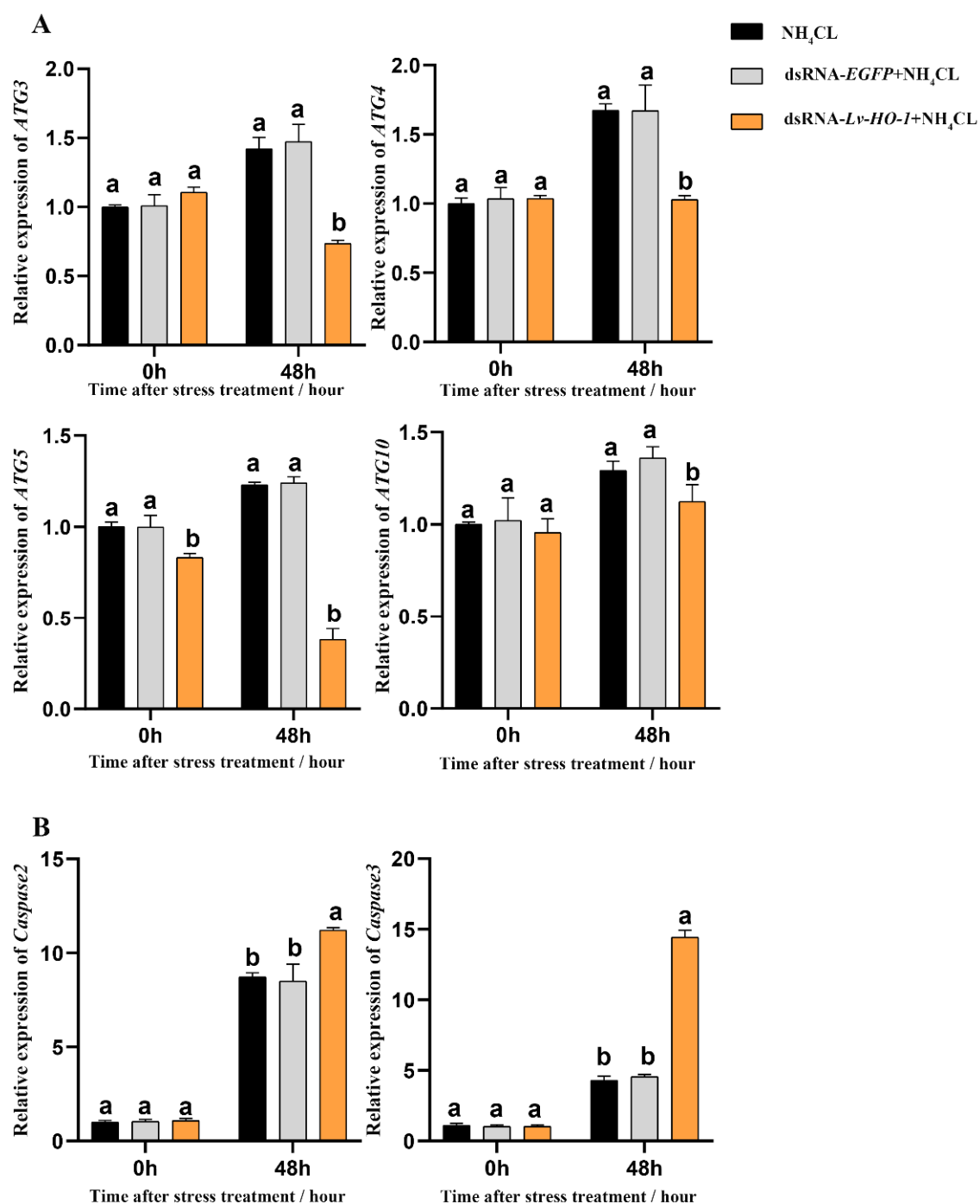


Figure 6. (A) Expression patterns of autophagy factors *Atg3*, *Atg 4*, *Atg 5*, and *Atg 10* as detected by qRT-PCR at different time points after ammonia exposure. (B) Expression patterns of apoptosis factors *caspase-2* and *caspase-3* as assessed via qRT-PCR at different time points after ammonia exposure. All values are the mean \pm SD; n = 3. Different letters indicate a significant difference ($p < 0.05$).

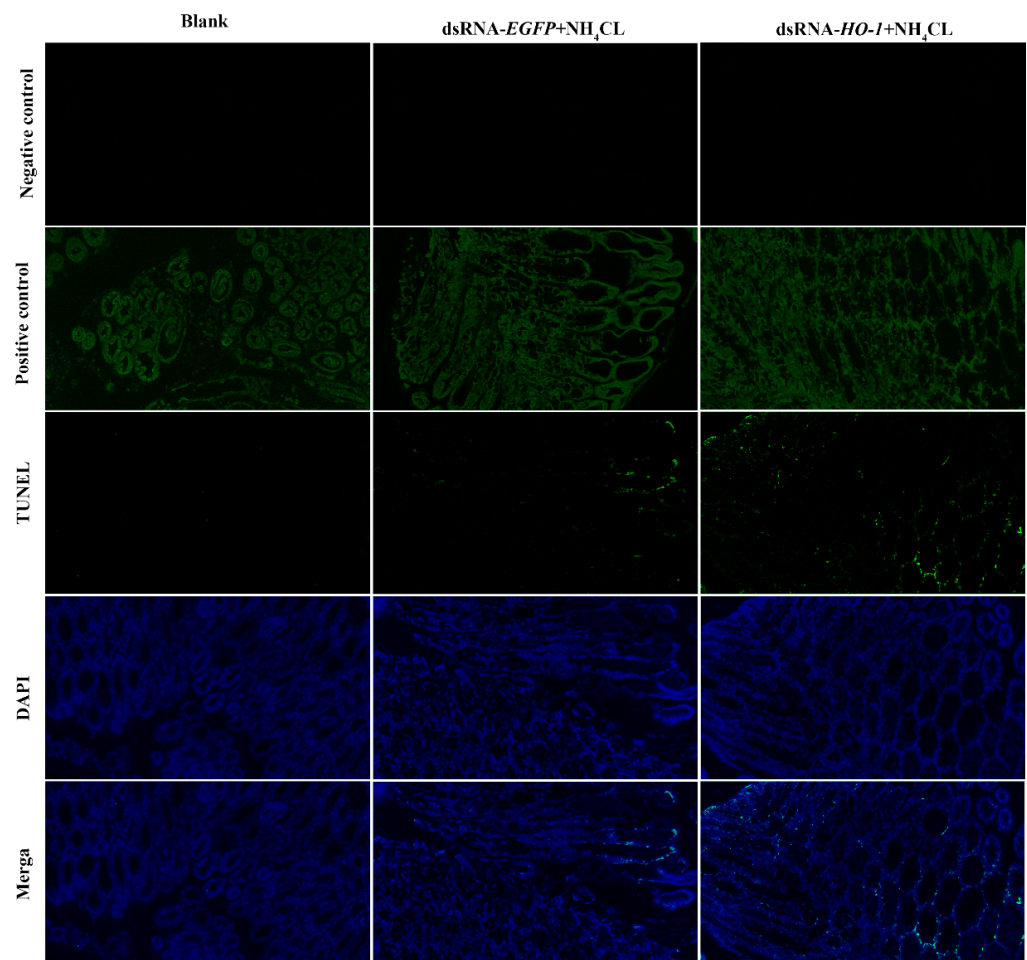


Figure 7. Apoptosis detection of intestine tissues of PBS group, dsRNA-EGFP+NH₄CL group, and dsRNA-HO-1+NH₄CL group at 48 h post-challenge via TUNEL assay. Apoptosis signals are marked in green. Nuclei are marked in blue. All sections were observed at 50× magnification.

4. Discussion

In this work, *Lv-HO-1* from *L. vannamei* was identified and characterized. The deduced *Lv-HO-1* is a membrane protein that contains a HemO structural domain. The HemO domain is the main activity domain for HO-1 and it is similar to *HO-1* found in eukaryotes and some bacteria [28–31]. More than 80% of other shrimp species and roughly 50% of insects share similarities with the deduced amino acid of *Lv-HO-1*. The result indicated that *Lv-HO-1* is preserved in a wide range of species. Phylogenetic tree analysis showed that *Lv-HO-1* is closely evolutionarily related to *P. monodon* and clustered with vertebrates.

In sea bass and swamp eel, the highest transcription level of *HO-1* was observed in the liver and was lower in other tissues [32,33]. Similarly, in golden pompano, the transcriptional level of *HO-1* was considerably high in the liver [34]. Furthermore, *HO-1* has also been shown to exhibit high levels of activity and gene expression in rat liver [35]. In this study, the expression levels of *Lv-HO-1* were mainly detected in the hepatopancreas, muscle, epidermis, and gill. Studies demonstrate that overexpressing *HO-1* reduces the replication of the hepatitis C virus (HCV) and oxidative liver damage [36]. In both mice and humans, deficiencies in *HO-1* expression can lead to chronic inflammatory states [37]. This observation is comprehensible because the hepatopancreas is the most vital detoxification and immune organ in an organism [38,39]. This finding suggested that *Lv-HO-1* may be involved in the immunological response to external stimuli.

Studies have shown that a high concentration of ammonia can induce oxidative stress by increasing the reactive oxygen species (ROS) in aquaculture animals [40]. Overproduc-

tion of ROS can harm lipids, proteins, and DNA [41]. Previous studies have proved that the juvenile liver of Nile tilapia suffered oxidative stress after being exposed to NH_3 for 72 days [42], and the antioxidant enzymes of *Penaeus vannamei* were dramatically increased first and then decreased, showing obvious cell fragmentation and vacuoles in hepatic tubules after ammonia exposure [21]. In the present study, *Lv-HO-1* expression considerably increased after ammonia-N stress. Furthermore, the expression level of *Lv-HO-1* peaked at 12 h in the hepatopancreas but peaked at 24 h in the muscle. In rats, *HO-1* was strongly expressed in the spleen and the liver [43]. Additionally, *HO-1* can be significantly increased in response to a variety of pro-oxidant and cellular stress-related stimuli, including ROS, nitric oxide, growth factors, free heme, and heavy metals, etc. [44]. In light of the fact that *HO-1* lessens tissue oxidative damage [45], it makes sense that *HO-1* increases rapidly as a stress protein in hepatopancreas and muscle under ammonia stress. Furthermore, the RNAi of *Lv-HO-1* showed that the expression levels of *Lv-HO-1* in hepatopancreas and muscle considerably decreased ($p < 0.05$) with a decreasing expression of *SOD* and *GSH-Px* genes and a decreasing enzyme activity of *SOD* compared with the control group after ammonia exposure. This result was consistent with the results from cattle ovarian granulosa cells, in that inhibition of *HO-1* expression by siRNA exacerbates oxidative stress after heat stress [46], which suggested that *HO-1* could regulate the antioxidant defense system of *L. vannamei* against oxidative stress.

In mammals, ROS accumulation contributes to abamectin-induced apoptosis and autophagy [47]. Autophagy can reduce the damage caused by oxidative stress in order to protect cells and increase lifespan [48]. Previous studies showed that after 42 days of ammonia treatment, chicken heart cells showed a clear autophagy phenomenon [49], and miR-252-mediated-ammonia-N-induced autophagy in *P. vannamei* [21].

Recent research has revealed that *HO-1* controls autophagy. In a model of RIPK, the inhibition of *HO-1* by Znpp decreased autophagy, aggravating liver damage [50]. *HO-1*^{-/-} mice also demonstrated that the autophagy genes *Atg5* and *Atg7* were inhibited, whereas *caspase-3* was significantly increased during cisplatin injury [51]. Another study reported that the knockdown of *HO-1* significantly increased cellular apoptosis in RAPA-treated cells [52]. A similar study in mice indicated that *HO-1* siRNA enhanced apoptosis via increased caspase 3 activity [53]. Our results showed that in an ammonia-nitrogen model, autophagy genes (*Atg3*, *Atg4*, *Atg5*, and *Atg10*) and apoptosis genes (*caspase-2* and *caspase-3*) can be significantly induced. The knockdown of *HO-1* shows a decrease in autophagy and instead exhibits higher levels of *caspase-2* and *caspase-3* and undergoes apoptosis more readily compared with the PBS group. Similar apoptosis results can also be derived from our TUNEL experiments. Moreover, MDA, an oxidative stress marker, exhibited higher content in the *HO-1*-RNAi group than in the control group. Additionally, stellate ductal dilatation and cellular atrophy were observed in the *HO-1*-RNAi group. Similar studies in rats indicated that the MDA content was regulated by *HO-1* during septic shock [54]. In previous studies, we demonstrated that when oxidative stress occurred, the oxidative damage of the body was increased due to the inhibition of the autophagy process, which led to an increase in apoptosis. These results indicated that *HO-1* can act as an antioxidant and autophagy regulator to protect cells from apoptosis [16,55].

5. Conclusions

In summary, shrimp *Heme Oxygenase-1* (*Lv-HO-1*) was identified and its involvement in oxidative stress was determined. In addition, the knockdown of *Lv-HO-1* is associated with a failure to further induce autophagy and leads to increased apoptosis after ammonia exposure. Furthermore, *Lv-HO-1* can be induced by oxidative stress and may have important roles in regulating the host antioxidant system, reducing cell apoptosis. This research offers a theoretical framework for further research on the mechanism of *HO-1* in shrimp.

Supplementary Materials: The following supporting information can be downloaded at: <https://www.mdpi.com/article/10.3390/fishes7060356/s1>, Table S1: The primers used in this research.

Author Contributions: Y.H.: Conceptualization, Data Curation, Writing—Original Draft; Q.L.: Conceptualization, Methodology; J.Z.: Resources; Z.Z.: Validation; Y.Y.: Resources; B.J.: Resources; J.L.: Resources; S.Y.: Project administration, Writing—Review and Editing; J.J.: Writing—Review and Editing, Funding acquisition. All authors have read and agreed to the published version of the manuscript.

Funding: This work was supported by the National Natural Science Foundation of China (No. U20A2065, 32073006, 32002426), National Key R&D Program of China (No. 2018YFD0900501), Project of the Agricultural Sci-tech Commissioners of Guangdong Province (KTP20210292), Fund of Southern Marine Science and Engineering Guangdong Laboratory (Zhanjiang) (No. ZJW-2019-06), Modern Seed Industry Park for Whiteleg Shrimp of Guangdong Province (K22219).

Institutional Review Board Statement: The animal study was reviewed and approved by Guangdong Province Laboratory Animal Management Regulations.

Data Availability Statement: Data is contained within the article and Supplementary Materials.

Acknowledgments: Thanks for the support of the Guangdong Provincial Key Laboratory of Aquatic Animal Disease Control and Healthy Culture & Key Laboratory of Control for Diseases of Aquatic Economic Animals of Guangdong Higher Education Institutes.

Conflicts of Interest: The authors declare that the research was conducted in the absence of any commercial or financial relationships that could be construed as a potential conflict of interest.

References

- Agarwal, A.; Nick, H.S. Renal response to tissue injury: Lessons from heme oxygenase-1 GeneAblation and expression. *J. Am. Soc. Nephrol.* **2000**, *11*, 965–973. [\[CrossRef\]](#)
- Maines, M.D.; Trakshel, G.M.; Kutty, R.K. Characterization of two constitutive forms of rat liver microsomal heme oxygenase. Only one molecular species of the enzyme is inducible. *J. Biol. Chem.* **1986**, *261*, 411–419. [\[CrossRef\]](#) [\[PubMed\]](#)
- Motterlini, R.; Foresti, R. Heme Oxygenase-1 As a Target for Drug Discovery. *Antioxid. Redox Signal.* **2014**, *20*, 1810–1826. [\[CrossRef\]](#) [\[PubMed\]](#)
- Li, C.; Stocker, R. Heme oxygenase and iron: From bacteria to humans. *Redox Rep.* **2009**, *14*, 95–101. [\[CrossRef\]](#)
- Czibik, G.; Derumeaux, G.; Sawaki, D.; Valen, G.; Motterlini, R. Heme oxygenase-1: An emerging therapeutic target to curb cardiac pathology. *Basic Res. Cardiol.* **2014**, *109*, 450. [\[CrossRef\]](#)
- Fang, X.; Wang, H.; Han, D.; Xie, E.; Yang, X.; Wei, J.; Gu, S.; Gao, F.; Zhu, N.; Yin, X.; et al. Ferroptosis as a target for protection against cardiomyopathy. *Proc. Natl. Acad. Sci. USA* **2019**, *116*, 2672–2680. [\[CrossRef\]](#)
- Maines, M.D. The Heme Oxygenase System: A Regulator of Second Messenger Gases. *Annu. Rev. Pharmacol. Toxicol.* **1997**, *37*, 517–554. [\[CrossRef\]](#) [\[PubMed\]](#)
- Hayashi, S.; Omata, Y.; Sakamoto, H.; Higashimoto, Y.; Hara, T.; Sagara, Y.; Noguchi, M. Characterization of rat heme oxygenase-3 gene. Implication of processed pseudogenes derived from heme oxygenase-2 gene. *Gene* **2004**, *336*, 241–250. [\[CrossRef\]](#)
- Silva, R.C.M.C.; Travassos, L.H.; Paiva, C.N.; Bozza, M.T. Heme oxygenase-1 in protozoan infections: A tale of resistance and disease tolerance. *PLoS Pathog.* **2020**, *16*, e1008599. [\[CrossRef\]](#) [\[PubMed\]](#)
- Shan, H.; Li, T.; Zhang, L.; Yang, R.; Li, Y.; Zhang, M.; Dong, Y.; Zhou, Y.; Xu, C.; Yang, B.; et al. Heme oxygenase-1 prevents heart against myocardial infarction by attenuating ischemic injury-induced cardiomyocytes senescence. *eBioMedicine* **2019**, *39*, 59–68. [\[CrossRef\]](#) [\[PubMed\]](#)
- Dulak, J.; Deshane, J.; Jozkowicz, A.; Agarwal, A. Heme Oxygenase-1 and Carbon Monoxide in Vascular Pathobiology. *Circulation* **2008**, *117*, 231–241. [\[CrossRef\]](#)
- Nath, K. Heme oxygenase-1: A provenance for cytoprotective pathways in the kidney and other tissues. *Kidney Int.* **2006**, *70*, 432–443. [\[CrossRef\]](#)
- Choi, A.M.; Alam, J. Heme oxygenase-1: Function, regulation, and implication of a novel stress-inducible protein in oxidant-induced lung injury. *Am. J. Respir. Cell Mol. Biol.* **1996**, *15*, 9–19. [\[CrossRef\]](#) [\[PubMed\]](#)
- Castilho, F.; Aveleira, C.A.; Leal, E.C.; Simões, N.F.; Fernandes, C.R.; Meirinhos, R.I.; Baptista, F.I.; Ambrósio, A.F. Heme Oxygenase-1 Protects Retinal Endothelial Cells against High Glucose- and Oxidative/Nitrosative Stress-Induced Toxicity. *PLoS ONE* **2012**, *7*, e42428. [\[CrossRef\]](#)
- Wiesel, P.; Patel, A.P.; DiFonzo, N.; Marria, P.B.; Sim, C.U.; Pellacani, A.; Maemura, K.; LeBlanc, B.W.; Marino, K.; Doerschuk, C.M.; et al. Endotoxin-Induced Mortality Is Related to Increased Oxidative Stress and End-Organ Dysfunction, Not Refractory Hypotension, in Heme Oxygenase-1-Deficient Mice. *Circulation* **2000**, *102*, 3015–3022. [\[CrossRef\]](#) [\[PubMed\]](#)
- Agarwal, A.; Balla, J.; Alam, J.; Croatt, A.J.; Nath, K.A. Induction of heme oxygenase in toxic renal injury: A protective role in cisplatin nephrotoxicity in the rat. *Kidney Int.* **1995**, *48*, 1298–1307. [\[CrossRef\]](#) [\[PubMed\]](#)
- Nath, K.A.; Haggard, J.J.; Croatt, A.J.; Grande, J.P.; Poss, K.D.; Alam, J. The Indispensability of Heme Oxygenase-1 in Protecting against Acute Heme Protein-Induced Toxicity in Vivo. *Am. J. Pathol.* **2000**, *156*, 1527–1535. [\[CrossRef\]](#)

18. Shiraishi, F.; Curtis, L.M.; Truong, L.; Poss, K.; Visner, G.A.; Madsen, K.; Nick, H.S.; Agarwal, A. Heme oxygenase-1 gene ablation or expression modulates cisplatin-induced renal tubular apoptosis. *Am. J. Physiol. Physiol.* **2000**, *278*, F726–F736. [[CrossRef](#)] [[PubMed](#)]
19. Tzaneva, V.; Perry, S.F. Heme Oxygenase-1 (Ho-1) Mediated Respiratory Responses to Hypoxia in the Goldfish. *Carassius Auratus. Respir. Physiol. Neurobiol.* **2014**, *199*, 1–8. [[CrossRef](#)]
20. Abaquita, T.A.L.; Damulewicz, M.; Bhattacharya, D.; Pyza, E. Regulation of Heme Oxygenase and Its Cross-Talks with Apoptosis and Autophagy under Different Conditions in *Drosophila*. *Antioxidants* **2021**, *10*, 1716. [[CrossRef](#)] [[PubMed](#)]
21. Wang, F.; Huang, L.; Liao, M.; Dong, W.; Liu, C.; Zhuang, X.; Liu, Y.; Yin, X.; Liang, Q.; Wang, W. Pva-miR-252 participates in ammonia nitrogen-induced oxidative stress by modulating autophagy in *Penaeus vannamei*. *Ecotoxicol. Environ. Saf.* **2021**, *225*, 112774. [[CrossRef](#)]
22. Zhang, L.; Pan, L.; Xu, L.; Si, L. Effects of ammonia-N exposure on the concentrations of neurotransmitters, hemocyte intracellular signaling pathways and immune responses in white shrimp *Litopenaeus vannamei*. *Fish Shellfish Immunol.* **2018**, *75*, 48–57. [[CrossRef](#)]
23. Si, L.; Pan, L.; Wang, H.; Zhang, X. Ammonia-N exposure alters neurohormone levels in the hemolymph and mRNA abundance of neurohormone receptors and associated downstream factors in the gills of *Litopenaeus vannamei*. *J. Exp. Biol.* **2019**, *222*, jeb.200204. [[CrossRef](#)] [[PubMed](#)]
24. Yang, S.; Huang, Y.; Chen, B.; Liu, H.; Huang, Y.; Cai, S.; Jian, J. Protective effects of sulphoraphane on oxidative damage caused by ammonia in *Litopenaeus vannamei*. *Aquac. Res.* **2022**, *53*, 1197–1204. [[CrossRef](#)]
25. Li, Q.; Zhang, Z.; Fan, W.; Huang, Y.; Niu, J.; Luo, G.; Liu, X.; Huang, Y.; Jian, J. LECT2 Protects Nile Tilapia (*Oreochromis niloticus*) Against *Streptococcus agalatae* Infection. *Front. Immunol.* **2021**, *12*, 667781. [[CrossRef](#)]
26. Li, Q.; Jiang, B.; Zhang, Z.; Huang, Y.; Xu, Z.; Chen, X.; Huang, Y.; Jian, J. SP protects Nile tilapia (*Oreochromis niloticus*) against acute *Streptococcus agalatae* infection. *Fish Shellfish Immunol.* **2022**, *123*, 218–228. [[CrossRef](#)]
27. Livak, K.J.; Schmittgen, T.D. Analysis of relative gene expression data using real-time quantitative PCR and the $2^{-\Delta\Delta CT}$ Method. *Methods* **2001**, *25*, 402–408. [[CrossRef](#)]
28. Shibahara, S.; Müller, R.; Taguchi, H.; Yoshida, T. Cloning and expression of cDNA for rat heme oxygenase. *Proc. Natl. Acad. Sci. USA* **1985**, *82*, 7865–7869. [[CrossRef](#)] [[PubMed](#)]
29. Evans, C.O.; Healey, J.F.; Greene, Y.; Bonkovsky, H.L. Cloning, sequencing and expression of cDNA for chick liver haem oxygenase. Comparison of avian and mammalian cDNAs and deduced proteins. *Biochem. J.* **1991**, *273*, 659–666. [[CrossRef](#)] [[PubMed](#)]
30. Rashid, I.; Baisvar, V.S.; Singh, M.; Kumar, R.; Srivastava, P.; Kushwaha, B.; Pathak, A.K. Isolation and characterization of hypoxia inducible heme oxygenase 1 (HMOX1) gene in *Labeo rohita*. *Genomics* **2020**, *112*, 2327–2333. [[CrossRef](#)]
31. Wilks, A.; Ikeda-Saito, M. Heme Utilization by Pathogenic Bacteria: Not All Pathways Lead to Biliverdin. *Acc. Chem. Res.* **2014**, *47*, 2291–2298. [[CrossRef](#)] [[PubMed](#)]
32. Zang, Y.; Zheng, S.; Tang, F.; Yang, L.; Wei, X.; Kong, D.; Sun, W.; Li, W. Heme oxygenase 1 plays a crucial role in swamp eel response to oxidative stress induced by cadmium exposure or *Aeromonas hydrophila* infection. *Fish Physiol. Biochem.* **2020**, *46*, 1947–1963. [[CrossRef](#)] [[PubMed](#)]
33. Prevot-D’Alvise, N.; Pierre, S.; Gaillard, S.; Gouze, E.; Gouze, J.-N.; Aubert, J.; Richard, S.; Grillasca, J.-P. cDNA sequencing and expression analysis of *Dicentrarchus labrax* heme oxygenase-1. *Cell Mol. Biol.* **2008**, *54*, O11046–O11054.
34. Xie, J.; He, X.; Fang, H.; Liao, S.; Liu, Y.; Tian, L.; Niu, J. Identification of heme oxygenase-1 from golden pompano (*Trachinotus ovatus*) and response of Nrf2/HO-1 signaling pathway to copper-induced oxidative stress. *Chemosphere* **2020**, *253*, 126654. [[CrossRef](#)] [[PubMed](#)]
35. Bauer, I.; Wanner, G.A.; Rensing, H.; Alte, C.; Miescher, E.A.; Wolf, B.; Pannen, B.H.J.; Clemens, M.G.; Bauer, M. Expression pattern of heme oxygenase isoenzymes 1 and 2 in normal and stress-exposed rat liver. *Hepatology* **1998**, *27*, 829–838. [[CrossRef](#)] [[PubMed](#)]
36. Zhu, Z.; Wilson, A.T.; Mathahs, M.M.; Wen, F.; Brown, K.E.; Luxon, B.A.; Schmidt, W.N. Heme oxygenase-1 suppresses hepatitis C virus replication and increases resistance of hepatocytes to oxidant injury. *Hepatology* **2008**, *48*, 1430–1439. [[CrossRef](#)] [[PubMed](#)]
37. Espinoza, J.A.; González, P.A.; Kalergis, A.M. Modulation of Antiviral Immunity by Heme Oxygenase-1. *Am. J. Pathol.* **2017**, *187*, 487–493. [[CrossRef](#)]
38. Röszer, T. The invertebrate midintestinal gland (“hepatopancreas”) is an evolutionary forerunner in the integration of immunity and metabolism. *Cell Tissue Res.* **2014**, *358*, 685–695. [[CrossRef](#)] [[PubMed](#)]
39. Diaz, A.C.; Gimenez, A.V.F.; Mendiara, S.N.; Fenucci, J.L. Antioxidant Activity in Hepatopancreas of the Shrimp (*Pleoticus muelleri*) by Electron Paramagnetic Spin Resonance Spectrometry. *J. Agric. Food Chem.* **2004**, *52*, 3189–3193. [[CrossRef](#)]
40. Liu, M.-J.; Guo, H.-Y.; Liu, B.; Zhu, K.-C.; Guo, L.; Liu, B.-S.; Zhang, N.; Yang, J.-W.; Jiang, S.-G.; Zhang, D.-C. Gill oxidative damage caused by acute ammonia stress was reduced through the HIF-1 α /NF-kb signaling pathway in golden pompano (*Trachinotus ovatus*). *Ecotoxicol. Environ. Saf.* **2021**, *222*, 112504. [[CrossRef](#)] [[PubMed](#)]
41. Zorov, D.B.; Juhaszova, M.; Sollott, S.J. Mitochondrial Reactive Oxygen Species (ROS) and ROS-Induced ROS Release. *Physiol. Rev.* **2014**, *94*, 909–950. [[CrossRef](#)] [[PubMed](#)]
42. Hegazi, M.M.; Attia, Z.I.; Ashour, O.A. Oxidative stress and antioxidant enzymes in liver and white muscle of Nile tilapia juveniles in chronic ammonia exposure. *Aquat. Toxicol.* **2010**, *99*, 118–125. [[CrossRef](#)] [[PubMed](#)]

43. Braggins, P.; Trakshel, G.; Kutty, R.; Maines, M. Characterization of two heme oxygenase isoforms in rat spleen: Comparison with the hematin-induced and constitutive isoforms of the liver. *Biochem. Biophys. Res. Commun.* **1986**, *141*, 528–533. [[CrossRef](#)] [[PubMed](#)]
44. Fredenburgh, L.E.; Merz, A.A.; Cheng, S. Haeme oxygenase signalling pathway: Implications for cardiovascular disease. *Eur. Heart J.* **2015**, *36*, 1512–1518. [[CrossRef](#)] [[PubMed](#)]
45. Zhang, M.; Zhang, B.H.; Chen, L.; An, W. Overexpression of heme oxygenase-1 protects smooth muscle cells against oxidative injury and inhibits cell proliferation. *Cell Res.* **2002**, *12*, 123–132. [[CrossRef](#)]
46. Wang, Y.; Yang, C.; Elsheikh, N.A.H.; Li, C.; Yang, F.; Wang, G.; Li, L. HO-1 reduces heat stress-induced apoptosis in bovine granulosa cells by suppressing oxidative stress. *Aging* **2019**, *11*, 5535–5547. [[CrossRef](#)]
47. Gur, C.; Kandemir, O.; Kandemir, F.M. Investigation of the effects of hesperidin administration on abamectin-induced testicular toxicity in rats through oxidative stress, endoplasmic reticulum stress, inflammation, apoptosis, autophagy, and JAK2/STAT3 pathways. *Environ. Toxicol.* **2022**, *37*, 401–412. [[CrossRef](#)] [[PubMed](#)]
48. Filomeni, G.; De Zio, D.; Cecconi, F. Oxidative stress and autophagy: The clash between damage and metabolic needs. *Cell Death Differ.* **2015**, *22*, 377–388. [[CrossRef](#)] [[PubMed](#)]
49. Xu, Y.; Li, Z.; Zhang, S.; Zhang, H.; Teng, X. miR-187-5p/apaf-1 axis was involved in oxidative stress-mediated apoptosis caused by ammonia via mitochondrial pathway in chicken livers. *Toxicol. Appl. Pharmacol.* **2019**, *388*, 114869. [[CrossRef](#)]
50. Wang, Y.; Shen, J.; Xiong, X.; Xu, Y.; Zhang, H.; Huang, C.; Tian, Y.; Jiao, C.; Wang, X.; Li, X. Remote Ischemic Preconditioning Protects against Liver Ischemia-Reperfusion Injury via Heme Oxygenase-1-Induced Autophagy. *PLoS ONE* **2014**, *9*, e98834. [[CrossRef](#)] [[PubMed](#)]
51. Bolisetty, S.; Traylor, A.M.; Kim, J.; Joseph, R.; Ricart, K.; Landar, A.; Agarwal, A. Heme Oxygenase-1 Inhibits Renal Tubular Macroautophagy in Acute Kidney Injury. *J. Am. Soc. Nephrol.* **2010**, *21*, 1702–1712. [[CrossRef](#)] [[PubMed](#)]
52. Banerjee, P.; Basu, A.; Wegiel, B.; Otterbein, L.E.; Mizumura, K.; Gasser, M.; Waaga-Gasser, A.M.; Choi, A.M.; Pal, S. Heme Oxygenase-1 Promotes Survival of Renal Cancer Cells through Modulation of Apoptosis- and Autophagy-regulating Molecules. *J. Biol. Chem.* **2012**, *287*, 32113–32123. [[CrossRef](#)] [[PubMed](#)]
53. Zhang, X.; Shan, P.; Jiang, D.; Noble, P.W.; Abraham, N.G.; Kappas, A.; Lee, P.J. Small Interfering RNA Targeting Heme Oxygenase-1 Enhances Ischemia-Reperfusion-induced Lung Apoptosis. *J. Biol. Chem.* **2004**, *279*, 10677–10684. [[CrossRef](#)] [[PubMed](#)]
54. Yu, J.-B.; Zhou, F.; Yao, S.-L.; Tang, Z.-H.; Wang, M.; Chen, H.-R. Effect of heme oxygenase-1 on the kidney during septic shock in rats. *Transl. Res.* **2009**, *153*, 283–287. [[CrossRef](#)] [[PubMed](#)]
55. Kim, H.P.; Wang, X.; Lee, S.-J.; Huang, M.-H.; Wan, Y.; Ryter, S.W.; Choi, A.M. Autophagic proteins regulate cigarette smoke induced apoptosis: Protective role of heme oxygenase-1. *Autophagy* **2008**, *4*, 887–895. [[CrossRef](#)] [[PubMed](#)]